SMiRT-12 / K. Kussmaul (Editor)
© 1993 Elsevier Science Publishers B.V. All rights reserved.

H05/1

STRUCTURAL INTEGRITY TESTS OF PRESTRESSED CONCRETE CONTAINMENT VESSELS AT OHI NUCLEAR POWER STATION

S. Setogawa, K. Sakurai, A. Funakoshi, T. Yamaguchi, K. Koike, I. Kamei and H. Hagio

ABSTRACT

This report describes structural integrity tests conducted on 2-buttress type prestressed concrete containment vessels (PCCVs) used for Units No.3 and 4 of Ohi Nuclear Power Station (ONPS) owned by The Kansai Electric Power Co., Inc.. The tests were carried out in order to confirm that the PCCVs were integral against the design pressure 4.0kgf/cm^2. The maximum test pressure was 4.5kgf/cm^2 (1.125 times the design pressure). Displacements, strains, temperatures and cracks of the PCCVs were measured. Based on the test results and evaluations, it was confirmed that the PCCVs hold sufficient structural integrity against the design pressure.

1 INTRODUCTION

For the first time in Japan, The Kansai Electric Power Co., Inc. has adopted 2-buttress type prestressed concrete containment vessels for Units No.3 and 4 (Pressurized Water Reactor, 1180 MW each) of ONPS. The structural integrity tests of these PCCVs were carried out in February 1991 and 1992, respectively. The purpose of the tests was to confirm that the PCCVs are integral against the design pressure.

2 OUTLINE OF PCCV

The configurations and dimensions of the two PCCVs, shown in Figure 1, are identical. The structure of each PCCV consists of a hemispherical dome, a cylindrical shell and a base mat. The hemispherical dome and the cylindrical shell are made of prestressed concrete, whereas reinforced concrete is used for the base mat. To achieve tightness against leakage, a steel liner is provided at the inside surface of the PCCV. The concrete structures of the PCCV are designed to assure pressure resistance and radiation shielding capability.

The inside radius and wall thickness of the hemispherical dome are 21.5m and 1.1m, respectively. For the cylindrical shell these parameters are 21.5m and 1.3m, respectively. The thickness of the base mat is 11.1m. The base mat has a tendon gallery to anchore inverted U tendons, while the hemispherical dome and the cylindrical shell have two vertical buttresses to anchore hoop tendons at 90° and 270°.

The design pressure is set to 4.0kgf/cm^2.

3 TESTING METHOD

3.1 Pressurization Method

The tests were performed simultaneously with the leak rate test according to the pressure variation relationship shown in Figure 2. The pressurization rate was about 0.1kgf/cm^2 per hour, and the maximum pressure of 4.54kgf/cm^2 was reached on the fourth day. The depressurization rate was about 0.2kgf/cm^2 per hour, and zero pressure was reached on the ninth day.

3.2 Measurement Method

Displacements, strains, temperatures and cracks of the PCCVs were measured.

The basic locations for measurement (A~L) are set at intervals of approximately 30° in plan as shown in Figure 3. Measurement locations (1~10) are distributed uniformly in the vertical direction over both the cylindrical portion and hemispherical dome. Thus, measurement locations are represented combining two symbols such as 4L.

With few exceptions measurements for Unit No.3 and 4 were conducted at the same locations. Listed below are the measurement items for Unit No.3.

1) Displacements

Displacements were measured using linear variable displacement transducers and super invar wires by the method shown in Figure 4. The arrangement of invar wires at mid-height of cylindrical wall, 4A to 4L, is shown in Figure 5.

2) Strains

Strains of the inside and outside reinforcing bars were measured to get membrane strains and bending strains in both, circumferential and meridian directions.

3) Temperatures

Temperatures of the PCCV structures were measured using thermocouples to revise thermal displacements and thermal strains. Air temperature was measured inside the PCCV and, inside and outside the reactor external building.

4) Inspection of Concrete Surface Crack

The locations of crack inspection zones are shown in Figure 6. Eight zones were selected considering stress conditions and easy access. Measurements were conducted before pressurization, in the midst of pressurization, at maximum pressure, in the midst of depressurization and after the end of depressurization.

4 METHOD OF ANALYSIS

4.1 Calculated Values From Design Models (δ_{c1})

Table 1 outlines the conditions for internal pressure design analysis for the PCCVs in Units No.3 and 4 of ONPS. The analysis was conducted using the following three models.

1) Overall model for general portion
2) Partial model with equipment hatch
3) Partial model with personal air lock

The design was based on 3-dimensional FEM elastic analysis, in which all structures were assumed made of concrete without steel. Young's modulus was assumed 3.15×10^5kgf/cm^2 corresponding to a specified concrete strength of 450kgf/cm^2, according to an equation proposed by the Architectural Institute of Japan.

Calculated displacements from design models were obtained using Equation (1). The stiffness of the actual PCCVs was evaluated considering: (1)-differences between Young's modulus at design stage and results obtained from compression tests on concrete pieces, (2)-steel stiffness and (3)-openings of tendon sheaths.

$$\left.\begin{aligned} \delta_{c1} &= \frac{E_D}{E_e}\cdot\delta_{co} \\ E_e &= \beta\cdot E_c\cdot\{1+(n-1)\,p_t\} \end{aligned}\right\} \quad\cdots\cdots (1)$$

where,

δ_{c1} : calculated displacement from design models using the actual stiffness

δ_{co} : design value of displacement

E_D : Young's modulus at design stage, 3.15×10^5kgf/cm^2

E_e : equivalent Young's modulus
4.08×10^5kgf/cm^2 (No.3), 3.76×10^5kgf/cm^2 (No.4)

E_c : Young's modulus of concrete test pieces collected from the actual PCCVs
4.18×10^5kgf/cm^2 (No.3), 3.81×10^5kgf/cm^2 (No.4)

β : stiffness degradation ratio due to openings of tendon sheaths, 0.9

n : ratio of Young's modulus, E_s/E_c, where $E_s=2.0\times10^6$kgf/cm^2

p_t : steel ratio in the circumferential direction at mid-height of a cylindrical wall, 0.0226 (representative)

Vertical displacements were measured with respect to the inner concrete structure which was taken as reference. Corresponding to this, for the purpose of analysis, vertical displacements of the PCCVs were added to vertical displacements of the inner concrete structure.

4.2 Calculated Values From Simulation Models (δ_{c2})

The main purpose of design analysis was to evaluate stresses, and the results were not sufficient to predict the deformation behavior of the PCCV in detail. Therefore, different types of elastic analysis were conducted by FEM models. In comparison with design models, the configurations of buttresses and equipment hatch were simulated by FEM models in a more realistic way. Calculated values from simulation models and calculated values from design models were obtained using the same stiffness evaluation method.

5 TEST RESULTS

5.1 Displacements

Representative internal pressure-displacement relationships for Unit No.3 respectively at the dome apex and the periphery of the equipment hatch are shown in Figures 7 and 8. The relationships show mostly elastic behavior of the PCCV with partial nonlinear behavior due to thermal displacement caused by changes of temperature. Some displacements changed during holding pressure at constant value and some yielded minus values at the end of depressurization. These phenomena are considered to arise from thermal deformation of the PCCVs and the inner concrete structures.

The average temperature variations of the PCCVs from the beginning of pressurization were relatively small, for example, -0.1 ℃ in Unit No.3 and +0.7℃ in Unit No.4 at maximum pressure. The average temperature variations were -1.3℃ in Unit No.3 and -2.1 ℃ in Unit No.4 at the end of depressurization. These temperature drops of the PCCV structures were caused by the drops of air temperature inside the PCCVs during depressurization.

5.2 Strains

Representative for Unit No.3 relationships between internal pressure and membrane strains in both meridian and circumferential directions are shown in Figure 9. Membrane strains are values calculated in the center of section from true strains not including strains caused by thermal stress. Each internal pressure-membrane strain relationship is almost linear.

5.3 Inspection of Concrete Surface Crack

From a structural viewpoint neither significant cracks nor unusual behavior of the PCCVs were observed. There were some cracks due to shrinkage before pressurization, but no one exceeded 0.2mm in width at maximum pressure.

6 EVALUATION RESULTS

6.1 Displacements at Maximum Pressure

Table 2 shows the comparison between measured and calculated displacements for Unit No.3 at maximum pressure. The following can be said from this table and the results for Unit No.4.

The ratios of measured values to values calculated by design models vary between 0.64 and 1.17 with an average value of 0.97 for Unit No.3, and between 0.72 and 1.09 with an average value of 0.93 for Unit No.4. On average, the measured values agree well with the calculated values, and consequently it becomes clear that the method for design analysis is appropriate. However, the above ratios are considerably different in each portion of the PCCV. For example, in buttress portions the average ratio values are 0.86 for Unit No.3 and 0.83 for Unit No.4. In the periphery of the equipment hatch the average ratio values are 0.83 for Unit No.3 and 0.75 for Unit No.4. And in all other portions- 1.07 for Unit No.3 and 1.00 for Unit No.4.

The ratios of measured values to values calculated by simulation models vary between 0.80 and 1.20 with an average value of 1.01 for Unit No.3, and between 0.75 and 1.09 with an average value of 0.95 for Unit No.4. The measured and calculated values coincide fairly well in every portion of the PCCV, too. For example, in buttress portions the average ratio values are 0.96 for Unit No.3 and 0.94 for Unit No.4. In the periphery of the equipment hatch the average ratio values are 0.99 for Unit No.3 and 0.94 for Unit No.4. And in all other portions- 1.04 for Unit No.3 and 0.96 for Unit No.4.

6.2 Comparisons of Displacement Distributions

Comparisons between measured and calculated displacement distributions at maximum pressure are shown in Figures 10 to 12. The results of the comparison are described in the following.

1) The measured and calculated values of radial displacement at cross section 4 of cylindrical wall coincide well as shown in Figure 10. However, values calculated by design models are higher than measured values in the buttress portions and the periphery of the equipment hatch.

2) Radial displacements at general longitudinal section H show good agreement between measured and calculated values as it can be seen from Figure 11.

3) On the whole, measured and calculated values of radial displacement at longitudinal section L coincide well as shown in Figure 12. However, above the equipment hatch the displacement value calculated by design models is higher than the measured value.

6.3 Displacements at the End of Depressurization

Table 3 shows a vertical displacement of the dome apex and eight radial displacements of cross section 4 for Unit No.3 at maximum pressure and at the end of depressurization. Thermal displacements were revised, because there were considerable temperature variations of the PCCV structures during depressurization. The average ratios of residual displacements to displacements at maximum pressure are 5% for both Unit No.3 and 4. Thus, it can be said that the PCCVs recover sufficiently from deformation caused by the internal pressure.

6.4 Membrane Strain Distributions

Comparisons of measured with calculated membrane strain distributions at maximum pressure are shown in Figures 13 to 15.

6.5 Correspondence of Displacements and Strains

Table 4 shows comparisons between the measured radial displacements and the products of the measured circumferential membrane strains multiplied by the radius of curvature. The average ratios of these products to measured radial displacements are 1.04 for Unit No.3 and 0.96 for Unit No.4. Correspondence of displacements and strains is fairly good, and shows that the measurement results are precise.

7 CONCLUSIONS

The following conclusions can be made:
1) The PCCVs behaved almost linearly, according to measured internal pressure-displacement relationships and pressure-membrane strain relationships.
2) From a structural viewpoint neither significant cracks nor unusual behavior of the PCCVs were observed.
3) When examining displacements and membrane strains at maximum pressure, the calculated values from design models agree well with measured values in general. Consequently it becomes clear that the design analysis is appropriate. Displacement values calculated by simulation models show good agreement with measured values in every portion of the PCCVs.

Based on the above test results and evaluations, it was confirmed that the PCCVs hold sufficient structural integrity against the design pressure.

REFERENCE

1) Tamura, S., Nagata, K., Takeda, T., Yamaguchi, T., and Nakayama, T. (1987). Structural Integrity Test of Prestressed Concrete Containment Vessel for Tsuruga Unit No.2 Nuclear Power Station. Transaction of the 9th SMiRT. Vol.J, pp.135-140

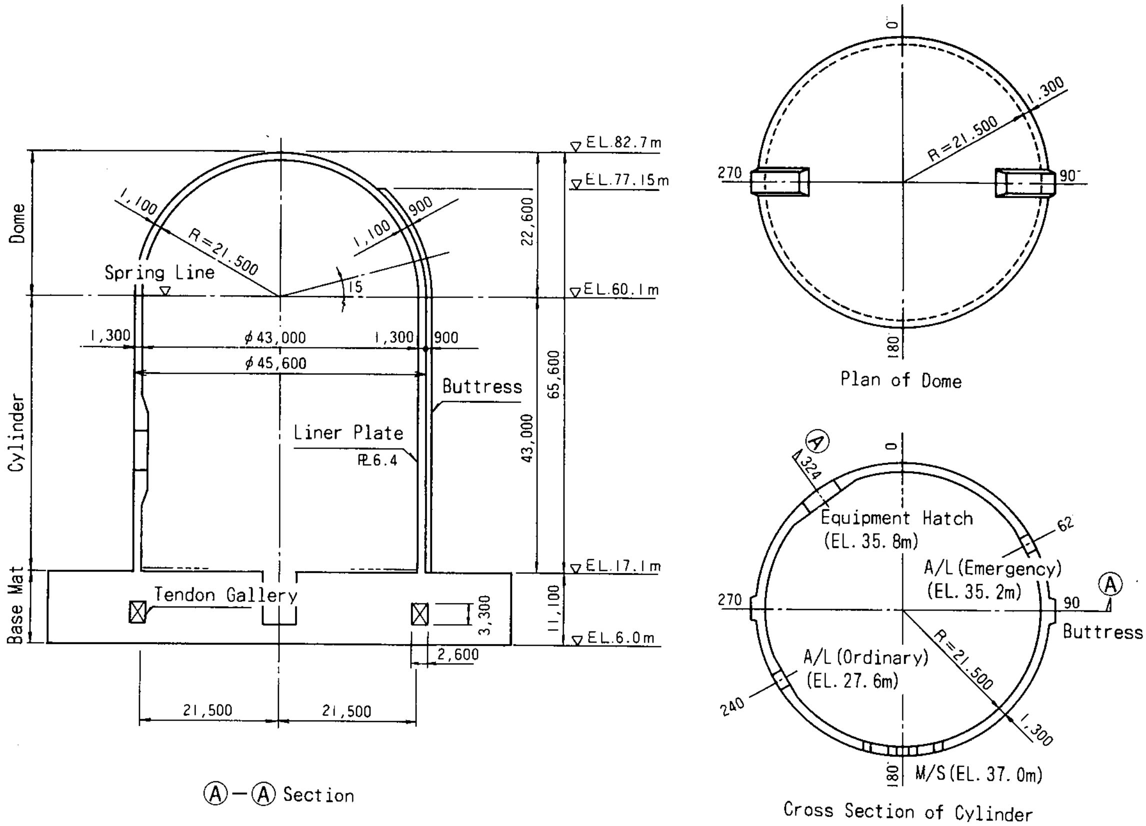

Fig.1 Outline of PCCV

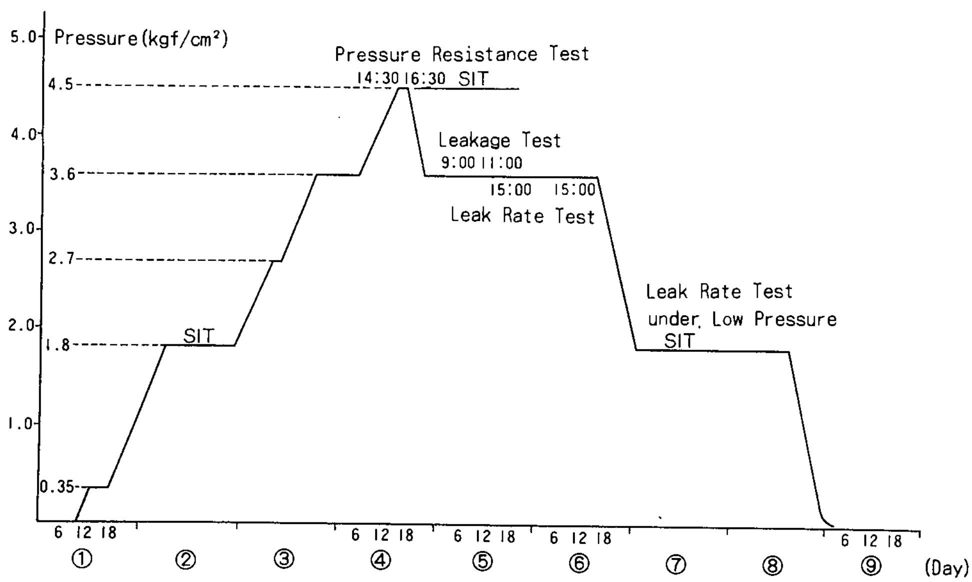

Fig.2 Pressure Variation Relationship

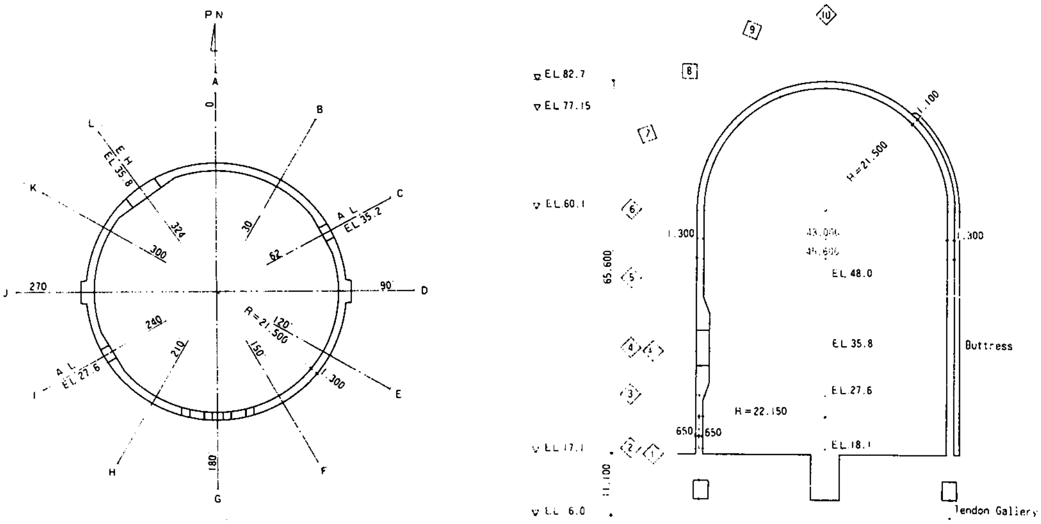

Fig. 3 Basic Location for Measurement

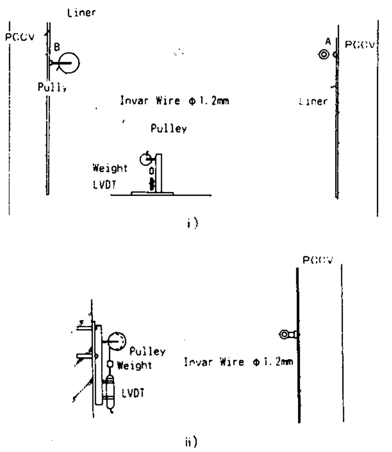

Fig. 4 Displacement Measurement Method

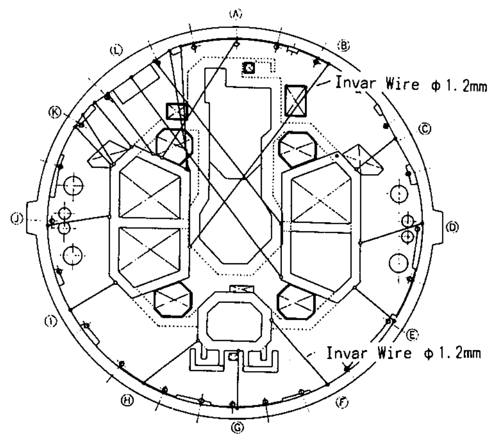

Fig. 5 Arrangement of Invar Wires

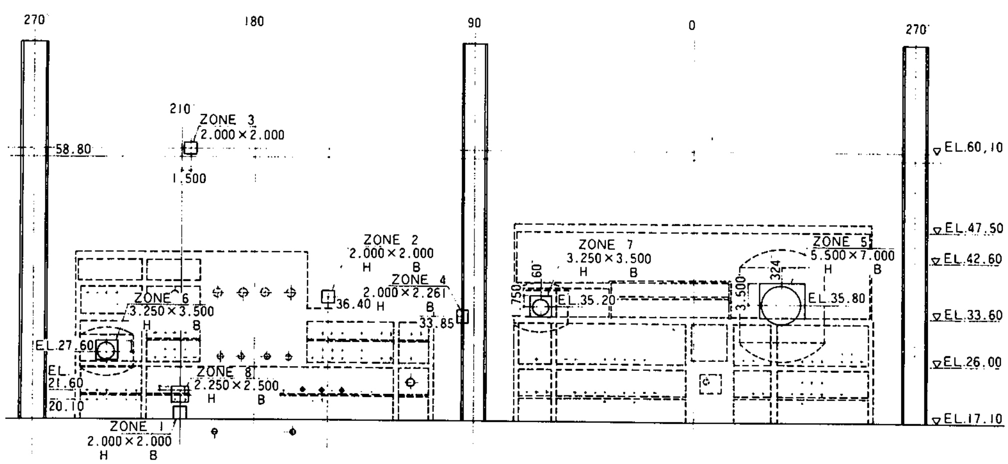

Fig. 6 Location of Crack Inspection Zones

Table 1 Conditions for Internal Pressure Design Analysis

	General portion	Large opening	
	Overall model	Partial model with E/H	Partial model with A/L
Code	SAP-V 3-dimensional FEM elastic analysis	Ditto	Ditto
Stiffness evaluation	All of structures are regarded as concrete with no steel.	Ditto	Ditto
Modeling	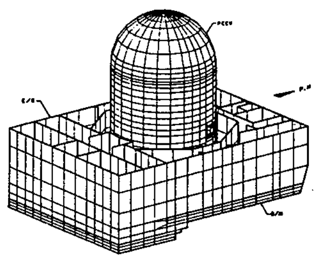 Overall model 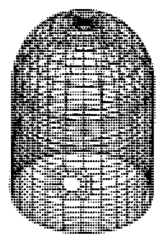 Shell portion of PCCV	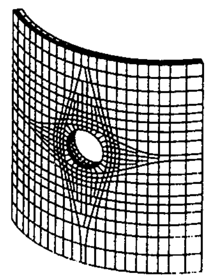	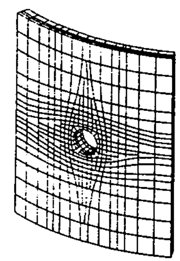
Material property	· PCCV and portion above tendon gallery : $E_c = 3.15 \times 10^5 kgf/cm^2$, $\nu = 0.167$ · Base mat : $E_c = 2.57 \times 10^5 kgf/cm^2$、 $\nu = 0.167$	$E_c = 3.15 \times 10^5 kgf/cm^2$ $\nu = 0.167$	$E_c = 3.15 \times 10^5 kgf/cm^2$ $\nu = 0.167$
Analytical conditions	· Internal pressure is distributed. · Bottom of shell is connected with base mat.	· Internal pressure is distributed. · Bottom is fixed. · Both sides are under symmetrical deformation condition. · Boundary load is input at upper end of cylinder.	Ditto

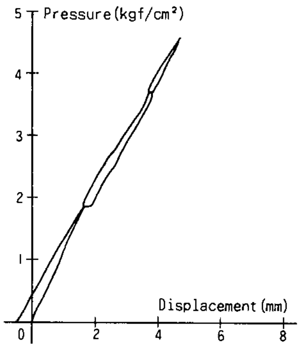

Fig. 7 Internal Pressure-Displacement Relationship (Dome Apex, Vertical)

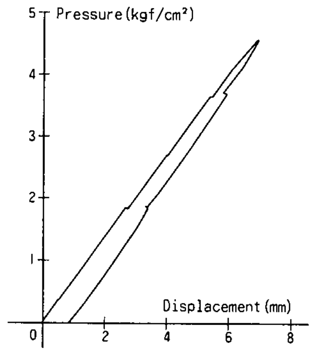

Fig. 8 Internal Pressure-Displacement Relationship (Periphery of E/H, Radial)

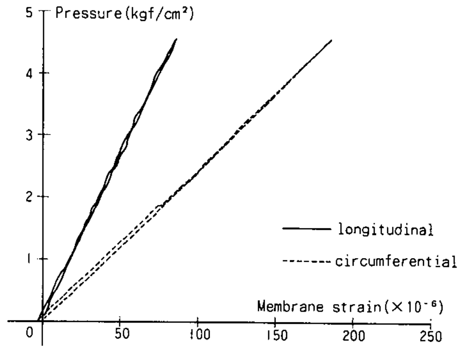

Fig. 9 Internal Pressure-Membrane Strain Relationship (General Portion of Cylinder, 4B)

Table 2 Displacements at Maximum Pressure ($4.54 kgf/cm^2$)

Location	Direction	Measured δ (mm)	Calculated δ_{c1} (mm)	δ_{c2} (mm)	Measured/Calcu. δ/δ_{c1}	δ/δ_{c2}
10L	Vertical	4.70	4.81	4.60	0.98	1.02
9L	Vertical	4.83	4.51	4.35	1.07	1.11
9FL	Radial*2	0.79	0.72	0.74	1.10	1.07
8D	Vertical	3.83	3.89	3.85	0.98	0.99
8JD	Radial*2	1.12	1.23	1.40	0.91	0.80
8H, 8L	Vertical	4.57	4.14	4.13	1.10	1.11
8BH, 8FL	Vertical	1.48	1.37	1.47	1.08	1.01
7L	Vertical	3.76	3.54	3.65	1.06	1.03
7FL	Radial*2	1.92	1.83	2.03	1.05	0.95
6D	Vertical	2.91	2.61	2.42	1.11	1.20
6JD	Radial	2.14	2.97	2.22	0.72	0.96
6H, 6L	Vertical	2.71	2.67	2.56	1.01	1.06
6BH, 6FL	Radial	3.82	3.64	3.91	1.05	0.98
5D	Vertical	2.17	2.23	2.25	0.97	0.96
5JD	Radial	2.09	3.27	2.38	0.64	0.88
5H, 5L	Vertical	2.64	2.26	2.45	1.17	1.08
5BH, 5FL	Radial	4.06	3.84	4.20	1.06	0.97
4A～4K*1	Radial	4.09	3.92	3.90	1.04	1.05
4D, 4J	Radial	2.37	3.36	2.44	0.71	0.97
4L	Radial	5.90	7.11	5.95	0.83	0.99
3D	Radial	2.55	3.12	2.73	0.82	0.93
3H	Radial	4.25	3.90	3.77	1.09	1.13

δ_{c1} : calculated values from design models
δ_{c2} : calculated values from simulation models
*1 : average value evaluated for nine points not including 4D and 4J
*2 : radial direction in horizontal section
(shaded) : buttress portion

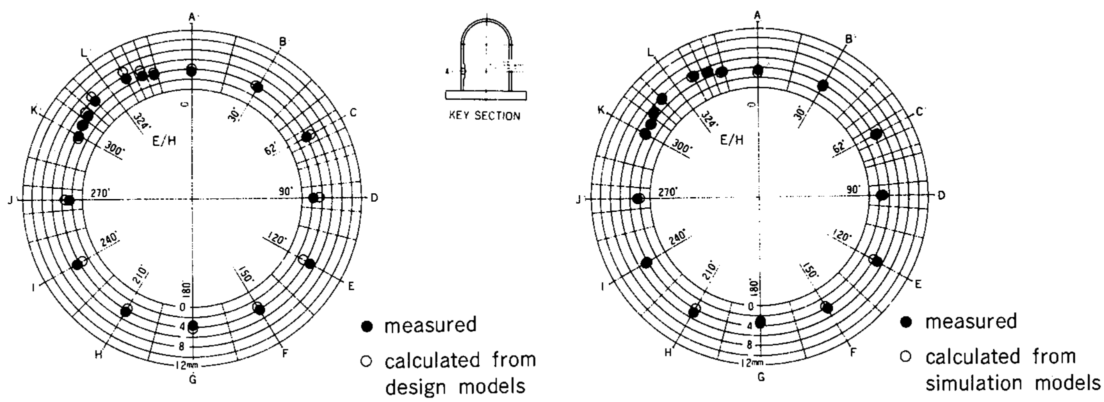

Fig. 10 Displacement Distribution (Section 4, Radial Direction)

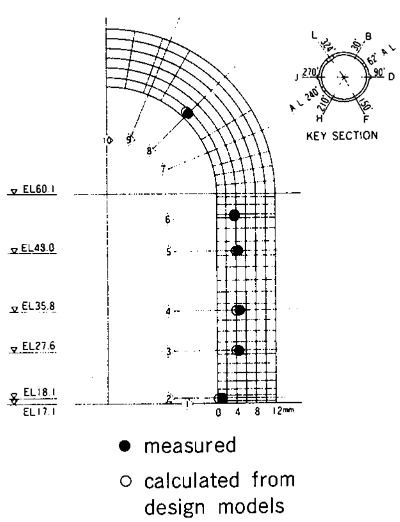

Fig. 11 Displacement Distribution (Section H, Radial Direction)

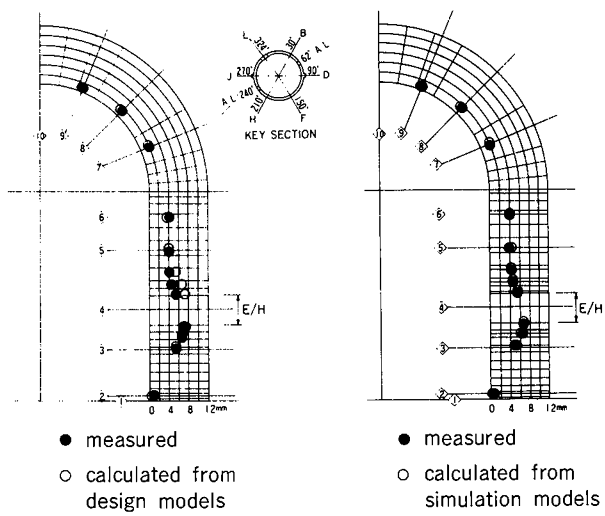

Fig. 12 Displacement Distribution (Section L, Radial Direction)

Table 3 Ratio of Residual Displacement to Displacement at Maximum Pressure

Location	Direction	Displacement at max.pres. δ_m (mm)	Residual displacement δ_o (mm)	δ_o/δ_m
10L	Vertical	4.70	0.36	0.08
4B	Radial	3.89	-0.13	-0.03
4E	Radial	5.07	0.64	0.13
4H	Radial	4.74	0.47	0.10
4K	Radial	3.74	0.02	0.01
4L-Left	Radial	5.71	0.03	0.01
4L-Right	Radial	5.75	0.37	0.06
4L-Above	Radial	5.46	0.12	0.02
4L-Below	Radial	6.66	0.49	0.07

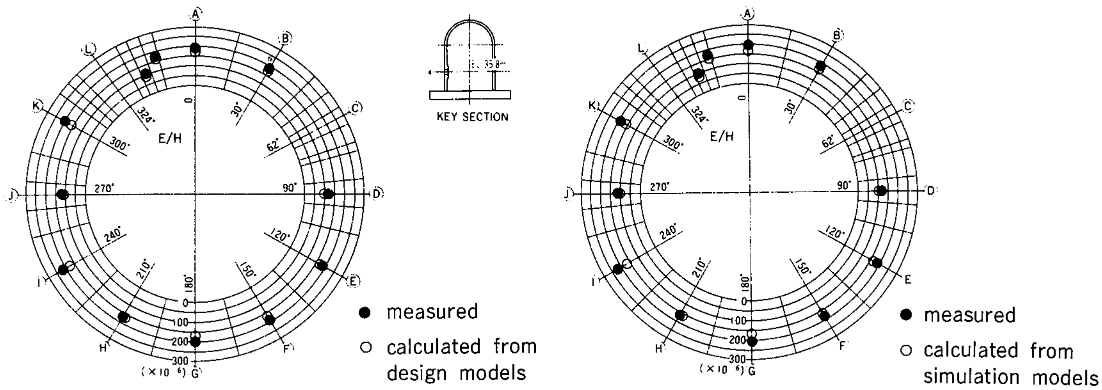

Fig. 13 Membrane Strain Distribution
(Section 4, Circumferential Direction)

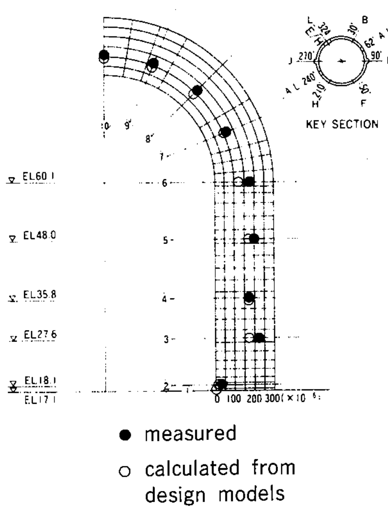

Fig. 14 Membrane Strain Distribution
(Section H, Circumferential Direction)

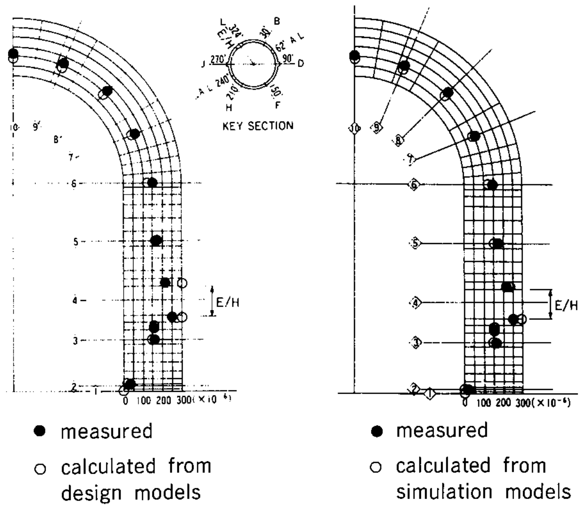

Fig. 15 Membrane Strain Distribution
(Section L, Circumferential Direction)

Table 4 Correspondence of Displacements and Strains

Location	Measured displacement δ (mm)	Measured strain ε ($\times 10^{-6}$)	Calculated displacement $\delta\varepsilon$ (mm)	$\delta\varepsilon / \delta$
9FL	0.79	107	0.90	1.14
8JD	1.12	68	1.12	1.00
8BH, 8FL	1.48	115	1.89	1.28
7FL	1.92	105	2.14	1.11
6JD	2.14	85	1.88	0.88
6BH, 6FL	3.82	161	3.57	0.93
5BH, 5FL	4.06	189	4.19	1.03
4A～4K*	4.09	193	4.27	1.04
4D, 4J	2.37	112	2.48	1.05
3D	2.55	112	2.48	0.97
3H	4.25	191	4.23	1.00
2D	0.31	20	0.44	1.42
2H, 2L	0.61	24	0.53	0.87

* : average value evaluated for nine points not including 4D and 4J